

## Article

# Basic Bio-Tribological Performance of Insulating Si<sub>3</sub>N<sub>4</sub>-Based Ceramic as Human Body Replacement Joints

Huaqiang Li <sup>1</sup>, Wei Chen <sup>2,\*</sup>, Hongxing Shi <sup>3</sup>, Chen Zhang <sup>1</sup>, Xingwei Liu <sup>1</sup> and Lisheng Zhong <sup>1,\*</sup>

<sup>1</sup> State Key Laboratory of Electrical Insulation and Power Equipment, Xi'an Jiaotong University, Xi'an 710049, China; lhqxjtu@xjtu.edu.cn (H.L.); zc.zgp.gy@stu.xjtu.edu.cn (C.Z.); lxw2018@stu.xjtu.edu.cn (X.L.)

<sup>2</sup> College of Mechanical and Electrical Engineering, Shaanxi University of Science & Technology, Xi'an 710021, China

<sup>3</sup> School of Mechanical Engineering, Southwest Jiaotong University, Chengdu 610031, China; shihx@my.swjtu.edu.cn

\* Correspondence: chenweijd@sust.edu.cn (W.C.); lszhong@xjtu.edu.cn (L.Z.)

**Abstract:** The paper presents an in-depth study of the bio-tribological performance on silicon nitride matrix ceramic composites containing hexagonal boron nitride (hBN) with different content. Ultra-high molecular weight polyethylene (UHMWPE) under simulated body fluid lubrication, and the simulated body fluid-lubricated sliding tests were performed on a universal friction and wear tester. The results showed that the incorporation of hBN into silicon nitride matrix reduced the friction coefficients from 0.27 for Si<sub>3</sub>N<sub>4</sub>/UHMWPE pair to 0.16 for Si<sub>3</sub>N<sub>4</sub>-20%hBN/UHMWPE with full immersion in simulated body fluid lubrication. Scanning electron microscopy (SEM), laser scanning microscope, X-ray photoelectron spectroscopy (XPS) were utilized to characterize the wear surface. The analysis results indicated that, with simulated body fluid lubrication, the interfacial between hBN and Si<sub>3</sub>N<sub>4</sub> facilitated the wear pits to form on the wear surface, and the residual wear particles deposited in the pits. Then, tribochemical products were formed on the wear surface, which protected and smoothed the wear surface of the sliding pair in the simulated body fluid.

**Keywords:** bio-tribology; silicon nitride based ceramic; simulated body fluid; tribochemical



**Citation:** Li, H.; Chen, W.; Shi, H.; Zhang, C.; Liu, X.; Zhong, L. Basic Bio-Tribological Performance of Insulating Si<sub>3</sub>N<sub>4</sub>-Based Ceramic as Human Body Replacement Joints. *Coatings* **2021**, *11*, 938. <https://doi.org/10.3390/coatings11080938>

Academic Editor: Alan Hase

Received: 22 June 2021

Accepted: 31 July 2021

Published: 5 August 2021

**Publisher's Note:** MDPI stays neutral with regard to jurisdictional claims in published maps and institutional affiliations.



**Copyright:** © 2021 by the authors. Licensee MDPI, Basel, Switzerland. This article is an open access article distributed under the terms and conditions of the Creative Commons Attribution (CC BY) license (<https://creativecommons.org/licenses/by/4.0/>).

## 1. Introduction

It is well known that, with the development of economy, technology and medicine, the mean lifespan of human constantly improve. Along with the extension of lifespan, the problem of osteoarthritis in aged becomes increasingly outstanding. Meanwhile, transportation accidents, industrial injuries and sport injuries may also bring about bone trauma [1]. Total hip arthroplasty is an effective means to relieve pain and improve the life quality of the patients with end-stage arthritis of the hip joint [2]. According to statistics, every year, no fewer than 300,000 hip arthroplasties have been performed in the United States, and 800,000 hip arthroplasties have been performed around the world.

Metal, polymer and ceramic could be all utilized as the hip replacement bearing materials. Meanwhile, titanium alloys (e.g., Ti6Al4V) and cobalt-chromium alloy have been used clinically due to good biocompatibility, avirulence, and their high strength and toughness. However, the free metal ions (e.g., cobalt ions) would diffuse in the tissues around the hip replacement, resulting in anaphylaxis [3]. Also, the metal replacement may induce some problems with stress shielding and medical image distortion. At the same time, it is well documented that polyethylene wear debris contributes to osteolysis, resulting in loosening of the prosthesis and ultimate failure [4,5]. Si [6] indicated that ultra-high molecular weight polyethylene UHMWPE was suited to acetabular components of hip joint and cushions, while UHMWPE could not be applied for total joint. Furthermore, bioceramic materials have been investigated for joint replacement because of their reduced

wear rates and an increased corrosion resistance, such as calcium phosphate materials [7,8], alumina ceramic [9] and zirconia [10]. However, brittleness fracture and poor machinability have been reported as major concerns for these ceramic materials.

Silicon nitride ( $\text{Si}_3\text{N}_4$ ) has been traditionally applied in engines, cutting tools and ball bearings due to its good mechanical performance [11]. During recent decades,  $\text{Si}_3\text{N}_4$  has been introduced into the biomedical field, e.g., used for spinal implants. In 2011, the first  $\text{Si}_3\text{N}_4$  femoral head was implanted in USA [12]. Why was  $\text{Si}_3\text{N}_4$  ceramic chosen as an implant material? It was motivated by its good biocompatibility, low wear and relatively high strength [13].

It is well known that, hexagonal boron nitride (hBN) is a kind of in-situ lubricating material with layered structure. The tribological properties and machinability of  $\text{Si}_3\text{N}_4$  ceramics can be further improved by adding hBN to the ceramic matrix [14–16]. Previously, scholars paid more attention to mechanical properties and tribological performance of  $\text{Si}_3\text{N}_4$ -hBN composites under engineering environment. Skopp [17] claimed that, for self-mated  $\text{Si}_3\text{N}_4$ -hBN composites in laboratory air, the tribochemical products of BN with water molecule were of benefit to the tribological performance of  $\text{Si}_3\text{N}_4$ -hBN composites in the range 22–150 °C. Meanwhile, Carrapichano [18] also reported hBN had a slight influence on proving anti-friction effect at room temperature. We [19,20] also found that, for  $\text{Si}_3\text{N}_4$ -hBN sliding pairs in laboratory, the incorporation of hBN into  $\text{Si}_3\text{N}_4$  ceramic resulted in a significant decrease of friction and wear, just because of the formation of tribochemical film. Generally, current research works mostly focus on the engineering tribological performance of  $\text{Si}_3\text{N}_4$ -based composites. In recent years, our team also focused on the bio-tribological properties, and found that addition of hBN significantly reduced the friction coefficient of  $\text{Si}_3\text{N}_4$ /TC4 bearing couple under simulated body fluid due to the formation of tribofilm [21]. It was also demonstrated that sliding velocity and contact load have obvious influence on the tribological behaviors of  $\text{Si}_3\text{N}_4$ -20%hBN/HXLPE bearing couple under simulated body fluid [22]. However, the influence of hBN content on the bio-tribological performance of  $\text{Si}_3\text{N}_4$ /HXLPE bearing couple under simulated body fluid has not been systematically studied. In particular, the anti-friction mechanism of hBN in  $\text{Si}_3\text{N}_4$ /HXLPE bearing couple still needs to be further deeply investigated under simulated body fluid.

At present paper, the tribological properties of  $\text{Si}_3\text{N}_4$ -hBN composite ceramics with different hBN contents sliding on UHMWPE were studied in simulated body fluid. Through measuring friction coefficient and wear rate, the biological friction properties of  $\text{Si}_3\text{N}_4$ -hBN/UHMWPE composites were analyzed and discussed. Meanwhile, the morphology of worn surface was observed, and the chemical composition was further analyzed. Moreover, the anti-friction of hBN was studied in this paper.

## 2. Experimental

### 2.1. Test Rig and Materials

The friction and wear of  $\text{Si}_3\text{N}_4$ -hBN/UHMWPE pair were carried out on a pin-on-disc tribological test rig. In this test rig, an upper pin slides against a stationary disc in simulated body fluid, and the wearing surface is fully immersed in the liquid. The schematic diagram of the equipment is shown in Figure 1. The fixed disc bears a normal load, and a strain gauge is used to continuously measure friction.

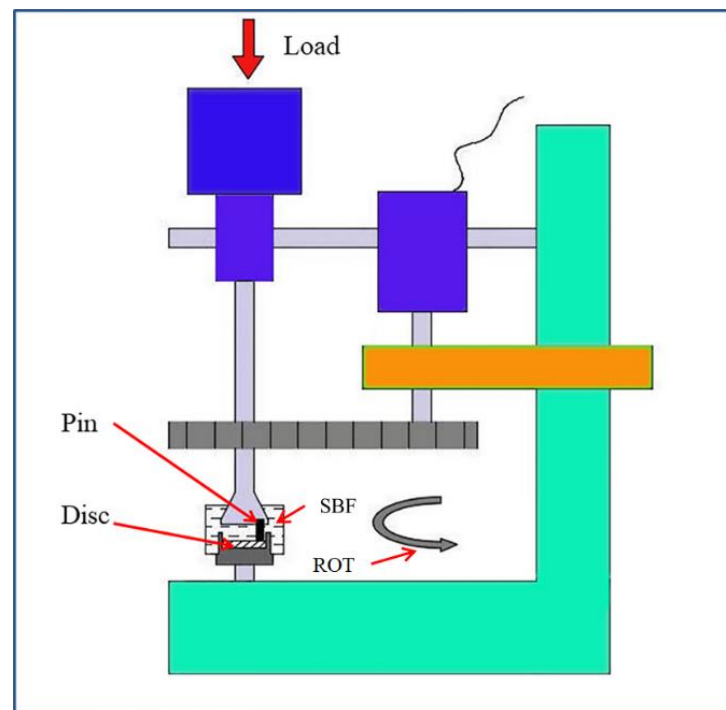


**Figure 1.** Schematic diagram of pin-on-disc testing machine.

Five types of  $\text{Si}_3\text{N}_4$  composite ceramics were hot-pressing sintered with varied hBN content of 0, 5, 10, 20 and 30 vol.% (corresponding to SN0, SN5, SN10, SN20 and SN30) under a pressure of 30MPa, at a temperature of 1800 °C for 30 min of dwell time. And Then, a ceramic disc with a size of  $\Phi 45 \text{ mm} \times 6 \text{ mm}$  was obtained. The blanks were sanded and cut into the required samples. The detailed preparation process has been given in our previous study [23]. Figure 2 illustrates the microstructures of the  $\text{Si}_3\text{N}_4$  composite ceramics. It can be seen that the pure  $\text{Si}_3\text{N}_4$  ceramic was mainly composed of elongated  $\beta\text{-Si}_3\text{N}_4$  grains (as shown in Figure 2a), and the composite ceramic was mainly composed of elongated  $\beta\text{-Si}_3\text{N}_4$  and lamellar hBN (as shown in Figure 2b–e). Meanwhile, when boron nitride (BN) was added to the  $\text{Si}_3\text{N}_4$  matrix, the densification of  $\text{Si}_3\text{N}_4$  ceramics decreased due to the interface inertia and the difference of thermal expansion coefficient. At the same time, because the boron nitride density is relatively low, the silicon nitride ceramic density decreased significantly.

In this study, the size of the pins (made of ceramic composite material) was 5 mm  $\times$  5 mm  $\times$  10 mm, with a rounded squared end to form a flat contact surface. In such a setting, the nominal contact area is approximately 22 mm<sup>2</sup>. The matching discs were made from UHMWPE material, which was purchased from Chunli Zhengda Medical Instruments Co. Ltd, Beijing, China. The size of disc was  $\Phi 44 \text{ mm} \times 6 \text{ mm}$ , and the surface roughness was around Ra 0.1  $\mu\text{m}$  by grinding. Meanwhile, the surface roughness of ceramic pin was around Ra 0.5  $\mu\text{m}$  by grinding utilized a diamond grinding tool. To adjust for the water-absorbing effects of the polymer, the disc sample was immersed in deionized water for about a month to achieve water saturation prior to the friction and wear test, according to Ref. [24]. SBF (simulated body fluid) liquid was prepared, according to Ref. [25]. Table 1 gives the corresponding ion concentrations and pH value, similar to those in human blood plasma.

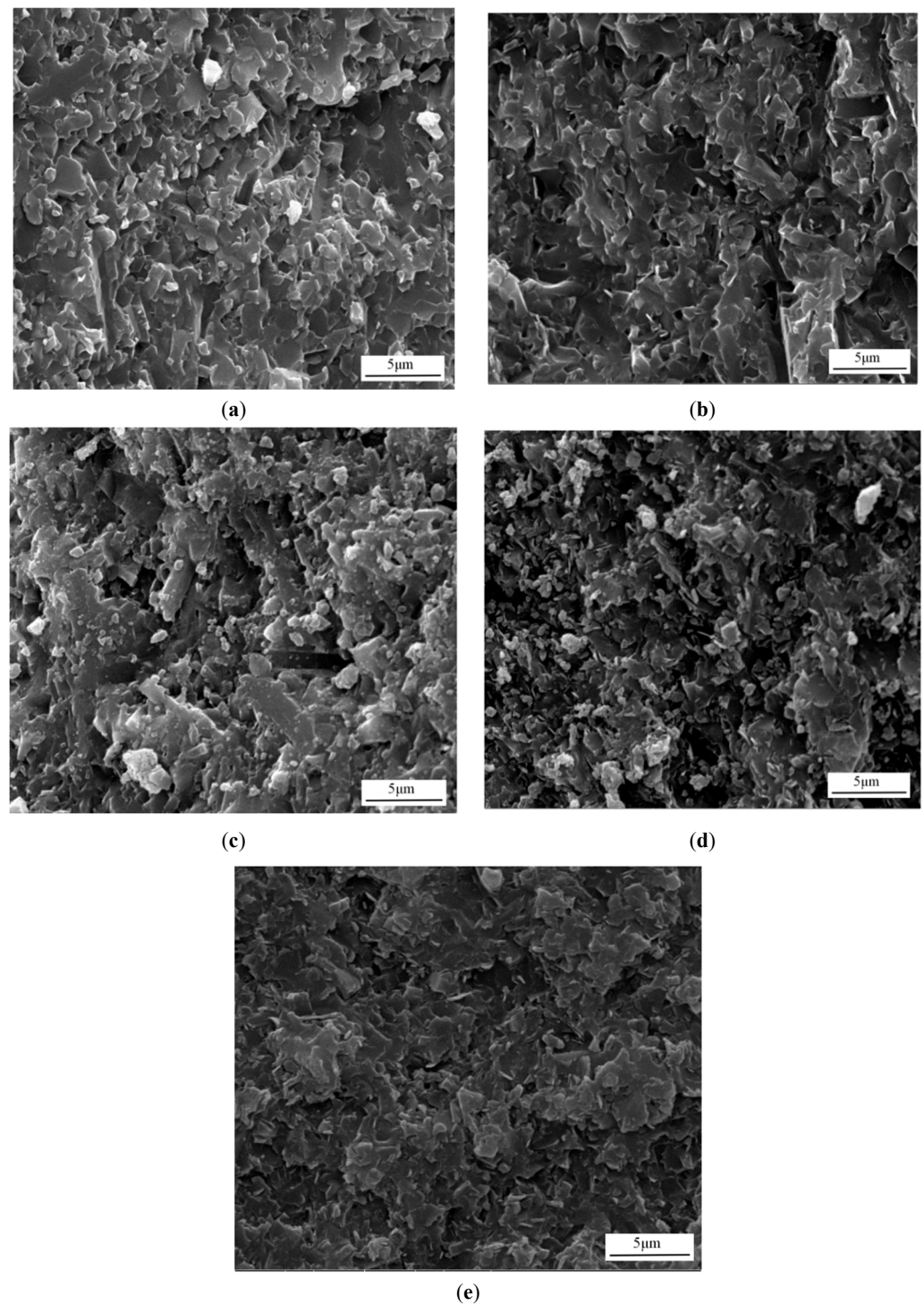


**Figure 2.** SEM image of fracture surface of (a) SN0, (b) SN5, (c) SN10, (d) SN20 and (e) SN30.

**Table 1.** Ion concentration of simulated body fluid (SBF) and plasma.

Constituents & pH	Na <sup>+</sup> (mmol/L)	K <sup>+</sup> (mmol/L)	Mg <sup>2+</sup> (mmol/L)	Ca <sup>2+</sup> (mmol/L)	Protein (g/L)	pH
Blood plasma [26]	142.0	5.0	1.5	2.5	64–83	7.2–7.4
SBF	142.0	5.0	1.5	2.5	0	7.4

## 2.2. Procedure

Before and after friction and wear tests, the samples needed to be cleaned, dried and weighed, according to Ref. [27]. Specifically, the samples were ultrasonic washed for minutes, and dried in the air. Then, the sample was weighed three times by electronic balance, and the average value was taken. Subsequently, all the tests were carried out in SBF at a speed of 500 r/min (0.73 m/s), normal load of 10 N, temperature of 36.5 °C, and a maximum sliding distance of 1000 m. Meanwhile, the nominal contact pressure from the normal load was 0.45 MPa. The initial running-in period was not considered when calculating the friction coefficient and wear rate. The friction coefficient  $f$  was directly given by the tester. The wear rate  $k$  was calculated by the following equation.

$$k = \Delta m / (\rho wx)$$

where,  $\Delta m$  represents the mass wear volume assessed by weight loss using a microbalance (accuracy = 0.1 mg),  $w$  is the normal load,  $x$  is the friction distance, and  $\rho$  is the density.

Three tribological tests were carried out for one test condition. Before and after each experiment, the silicon nitride ceramic composite pin and polymer disc were weighed three times, and the average value was taken. The morphology of the worn surface was observed by SEM, and the chemical characterization was analyzed by EDS (Energy Dispersive Spectrometer) and XPS (X-ray Photoelectron Spectroscopy).

## 3. Results and Discussion

Figure 3 illustrated the friction coefficients and wear rates of Si<sub>3</sub>N<sub>4</sub>-hBN/UHMWPE pair under SBF lubrication. Figure 3a indicates the friction coefficients of the specimens at a sliding distance of 1000 m. The incorporation of hBN reduced the friction coefficient from 0.27 for SN0/UHMWPE pair to 0.16 for SN20/UHMWPE pair. Figure 3b presents the wear rates of UHMWPE discs. In this study, the wear rates of Si<sub>3</sub>N<sub>4</sub>-hBN pin were too small to detect them. Obviously, the wear of the friction pairs was mainly originated from the wear loss of UHMWPE disc. From Figure 3, it can be easily found that, the best results were exhibited for the SN20/UHMWPE pair in SBF.

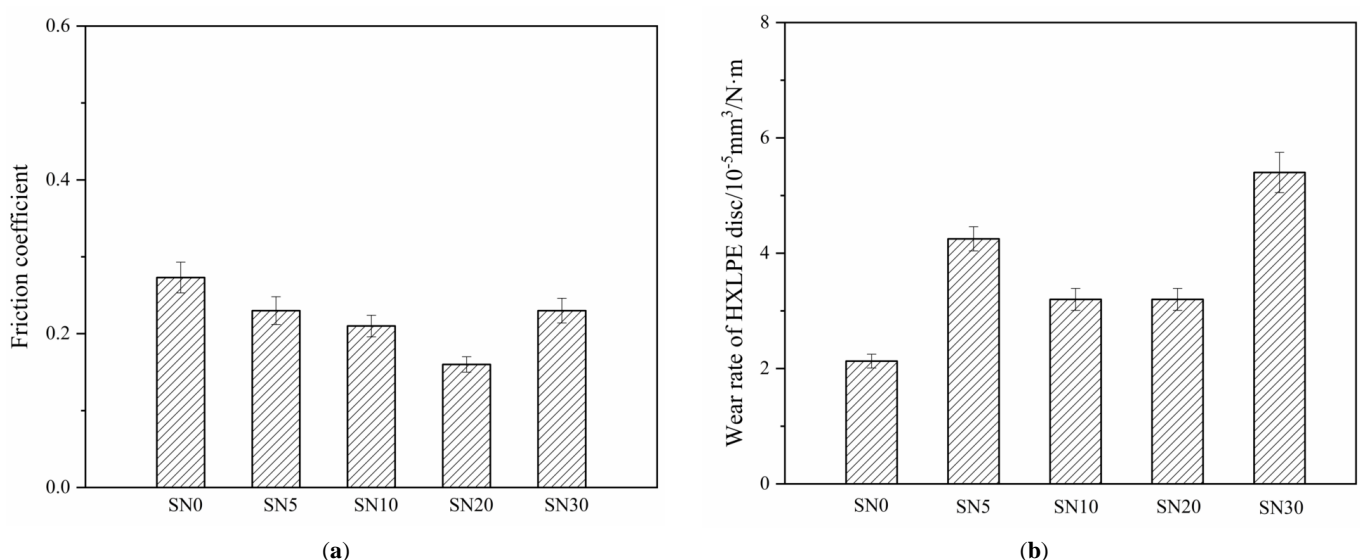
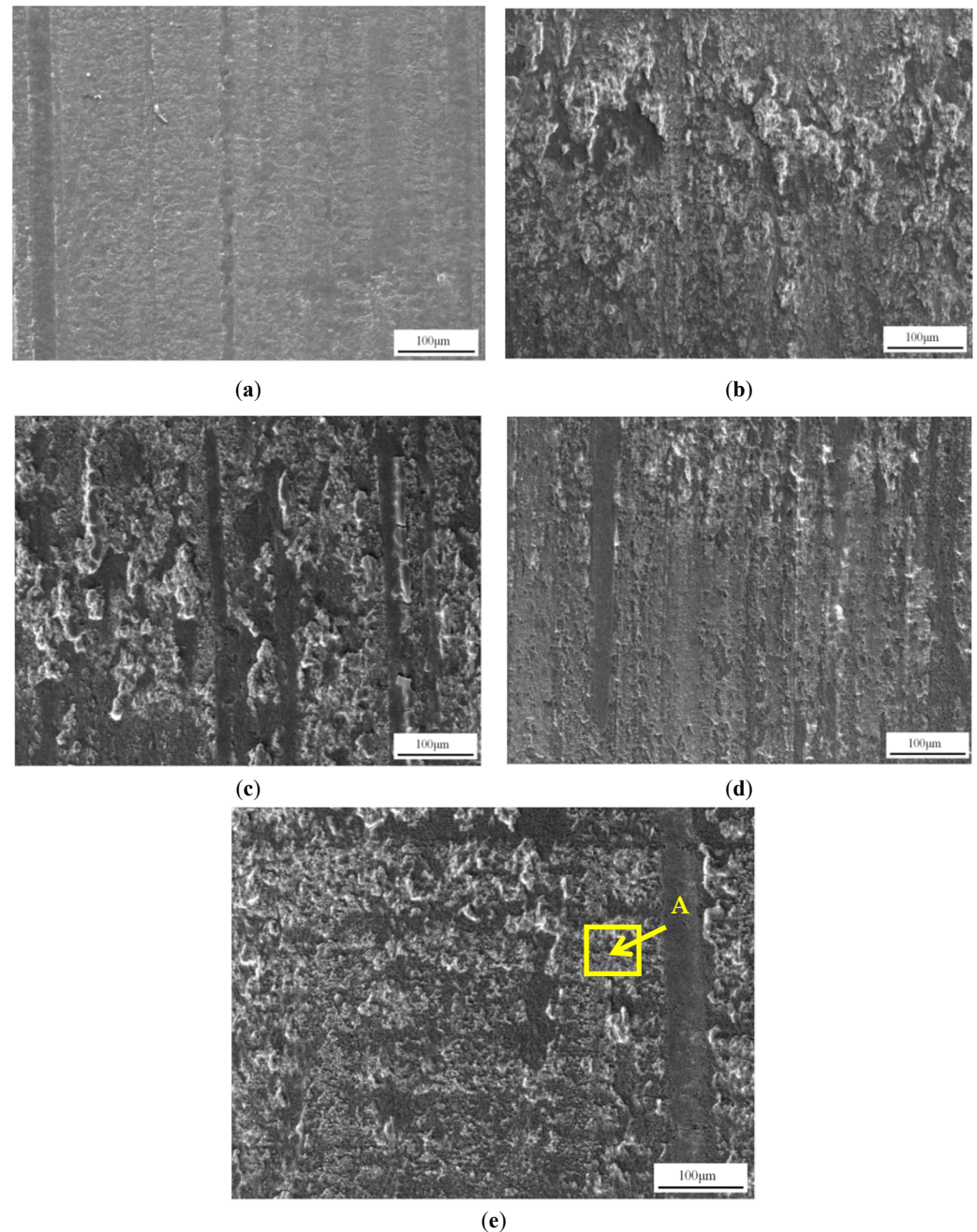


Figure 3. (a) Friction coefficients of Si<sub>3</sub>N<sub>4</sub>-hBN/UHMWPE pairs in SBF and (b) the wear rates of UHMWPE discs.

Figure 4 gives the SEM images of morphologies of the ceramic composite pins against UHMWPE in SBF lubricant. From the figure, the worn surfaces present great alteration with hBN content increasing. SEM observation of the pure Si<sub>3</sub>N<sub>4</sub> ceramic pin manifests a slightly rough surface. With the increase of hBN content, the surface gradually became rougher

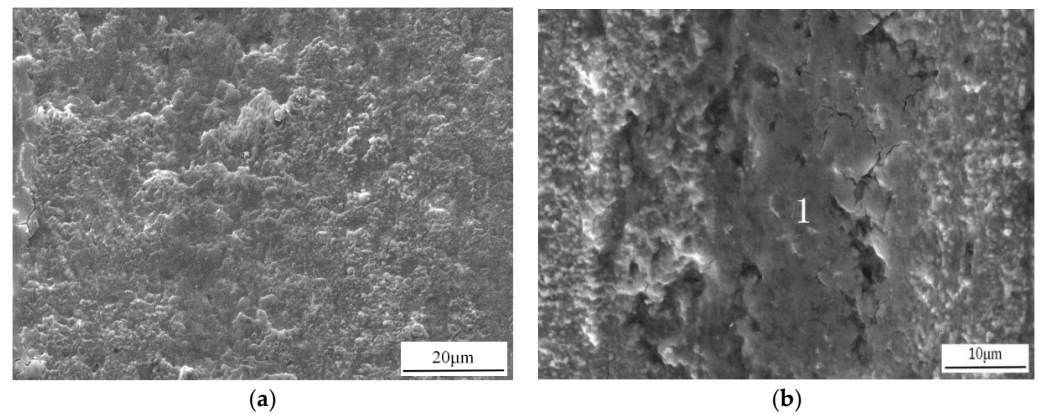
and rougher. Meanwhile, the worn surface of  $\text{Si}_3\text{N}_4$ -20%hBN pin manifests a relatively smoother surface, which is composed of a smoother surface (area “A” in Figure 4d) and rough surface. The composite pin surface becomes rough once again with excessive hBN content of 30%.



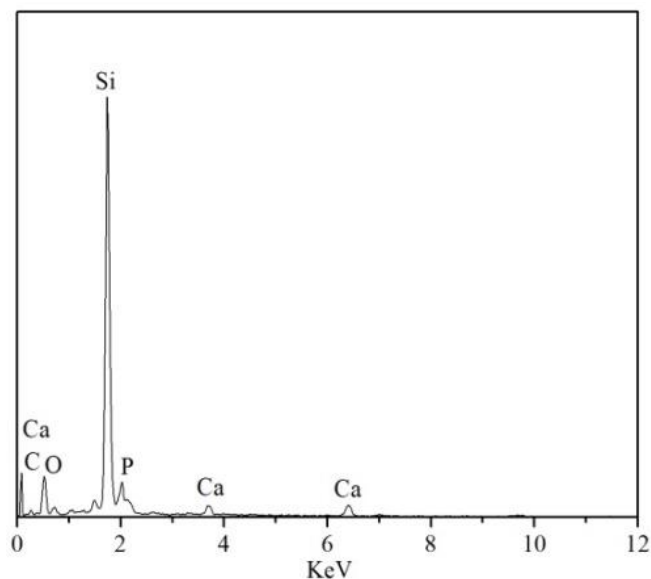
**Figure 4.** Worn surfaces of  $\text{Si}_3\text{N}_4$ -hBN composites pins against UHMWPE disc in SBF: (a) SN0 pin; (b) SN5 pin; (c) SN10 pin; (d) SN20 pin; (e) SN30 pin.

Figure 5 shows the high magnification image of the pin surfaces of pure  $\text{Si}_3\text{N}_4$  ceramic and  $\text{Si}_3\text{N}_4$ -20%hBN composite. Figure 5a denotes that the worn surface morphology of pure  $\text{Si}_3\text{N}_4$  pin is covered by adherent wear debris layers, and some loose particles and fracture can be also observed. Figure 5b gives the high magnification of area “A” in the pin surface of  $\text{Si}_3\text{N}_4$ -20%hBN composite. From this figure, some smooth area can be further observed. EDS analysis results of the smooth area (area “1”) on the worn surface of  $\text{Si}_3\text{N}_4$ -

20%hBN pin are shown in Figure 6. From the figure, oxygen atom, silicon atom and calcium atom can be found in the worn surface.



**Figure 5.** High magnification image of the worn surface for (a) SN0 pin sample and (b) SN20 pin sample against UHMWPE under SBF lubrication.



**Figure 6.** EDS analysis results of SN20 pin against UHMWPE disc (point 1).

The  $\text{Si}_3\text{N}_4$ -20%hBN pin surface after sliding against UHMWPE disc was analyzed by using XPS. Figure 7 shows that the  $\text{B}_{1s}$  and  $\text{Si}_{2p}$  peaks on the worn surface can be decomposed into two peaks, respectively. According to the relevant standard, from Figure 7a, one is 193.6 eV, which is close to 193.1 corresponding to  $\text{B}_2\text{O}_3$ ; the other is 192.2 eV, which corresponds to  $\text{H}_3\text{BO}_3$ . Meanwhile, the  $\text{Si}_{2p}$  peak can also be decomposed into two peaks (Figure 7b), which correspond to  $\text{SiO}_2$  and  $\text{Si}_3\text{N}_4$  respectively. Thus, it may be concluded that some tribo-chemical products (especially in the smooth area “A” in Figure 4d) formed during the friction process. This phenomenon was also found in our previous studies [19,20].

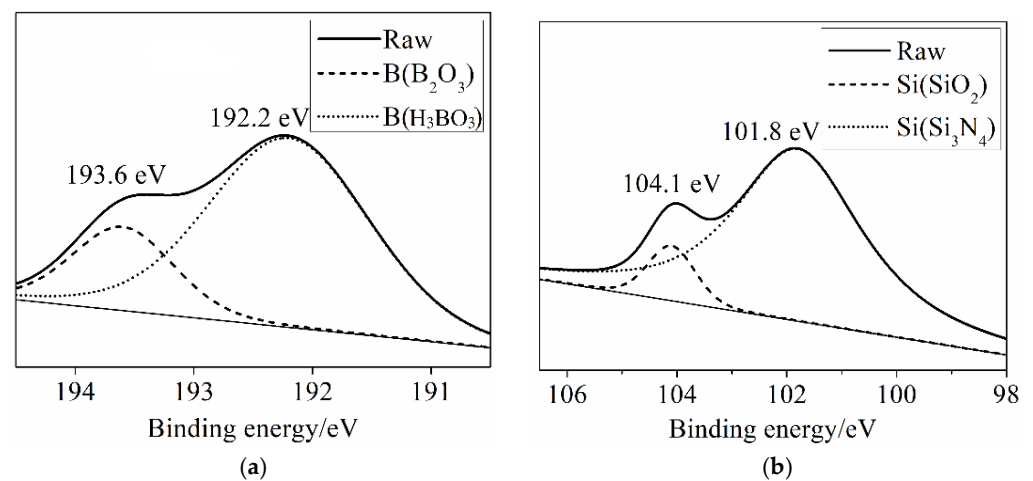


**Figure 7.** Binding energy on the worn surface of SN20 pin against UHMWPE disc in SBF: (a) B 1s and (b) Si 2p.

In our previous studies [28], it was verified that Si<sub>3</sub>N<sub>4</sub> and BN could react with water molecules during the friction process. The incorporation of hBN into Si<sub>3</sub>N<sub>4</sub> matrix was beneficial to provide some storage space for the tribochemical products and induce the formation of a film. In this study, the obvious tribofilm was not found on the worn surfaces of pin samples. However, some tribochemical products were detected on the worn surface of Si<sub>3</sub>N<sub>4</sub>-20%hBN pin. In particular, the Si<sub>3</sub>N<sub>4</sub>-20%hBN pin against UHMWPE disc shows a polyphyletic morphology composed of rough surface and smooth surface. Meanwhile, the Si<sub>3</sub>N<sub>4</sub>-20%hBN/UHMWPE pair shows better tribological characteristics.

Figure 8 shows the SEM morphologies of worn surfaces of UHMWPE discs against different ceramic pins. From the figures, it can be clearly found that some fine particles adhere to the worn surface of the UHMWPE disc against the pure Si<sub>3</sub>N<sub>4</sub> pin, and the furrow morphology can be observed. When the UHMWPE disc slid against Si<sub>3</sub>N<sub>4</sub>-5%hBN and Si<sub>3</sub>N<sub>4</sub>-10%hBN, the disc presented a significant deformation and fracture feature, and surfaces became rougher. When the UHMWPE disc slid against Si<sub>3</sub>N<sub>4</sub>-20%hBN pin, the disc surface was relatively smooth, and obvious furrow morphology could be also observed. However, when the UHMWPE disc slid against the Si<sub>3</sub>N<sub>4</sub>-30%hBN pin, the disc surface again became rougher. The corresponding 3-D images of the UHMWPE discs against Si<sub>3</sub>N<sub>4</sub>, Si<sub>3</sub>N<sub>4</sub>-20%hBN and Si<sub>3</sub>N<sub>4</sub>-30%hBN are shown in Figure 9.

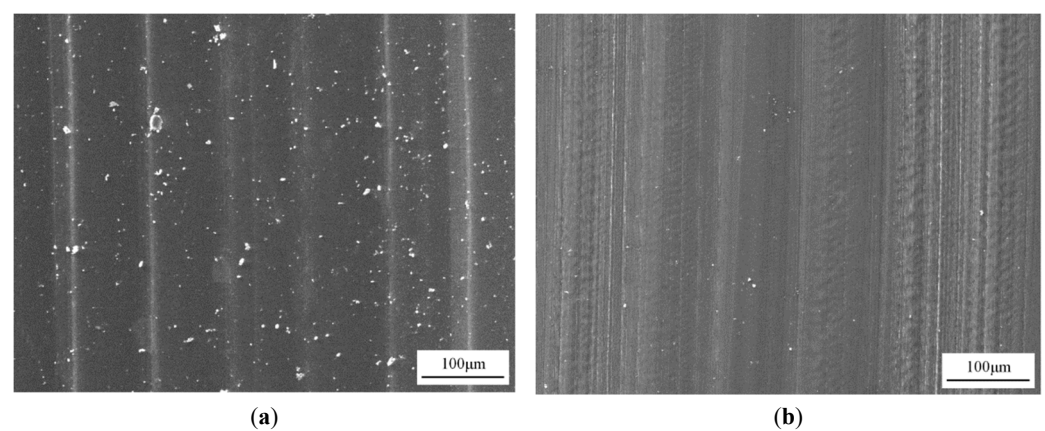


**Figure 8.** Cont.

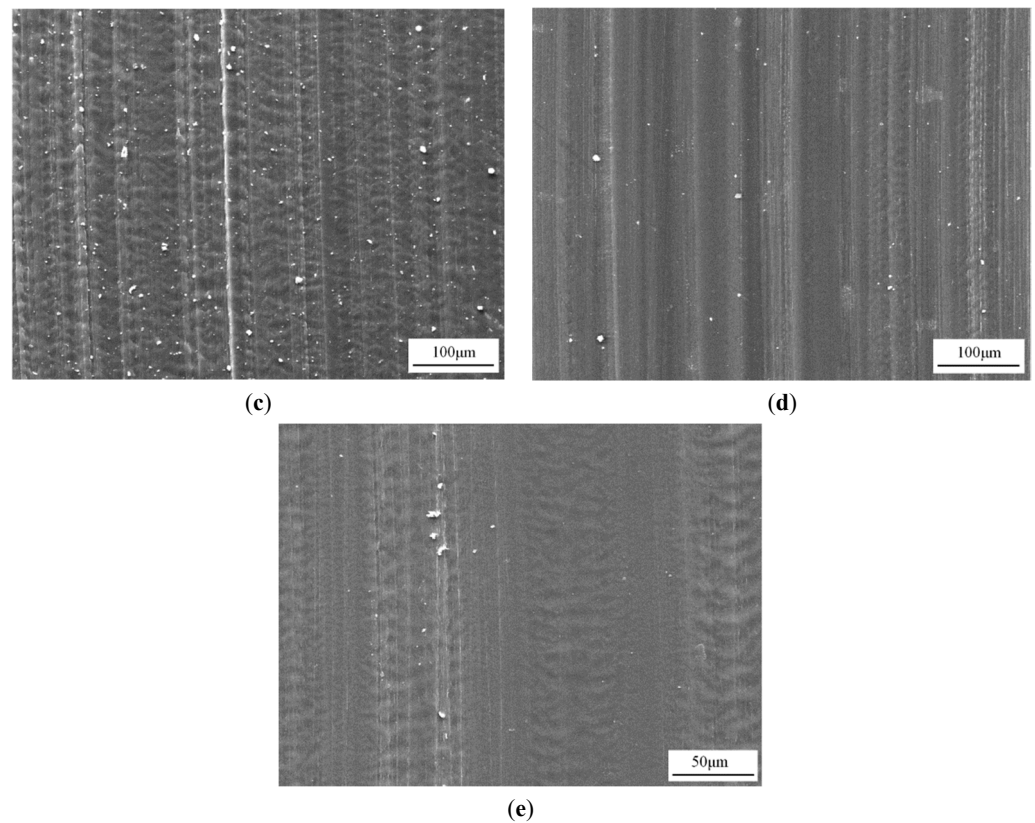


**Figure 8.** Worn surfaces of UHMWPE discs sliding against  $\text{Si}_3\text{N}_4$ -hBN composites in SBF: (a) against SN0 pin; (b) against SN5 pin; (c) against SN10 pin; (d) against SN20 pin; (e) against SN30 pin.

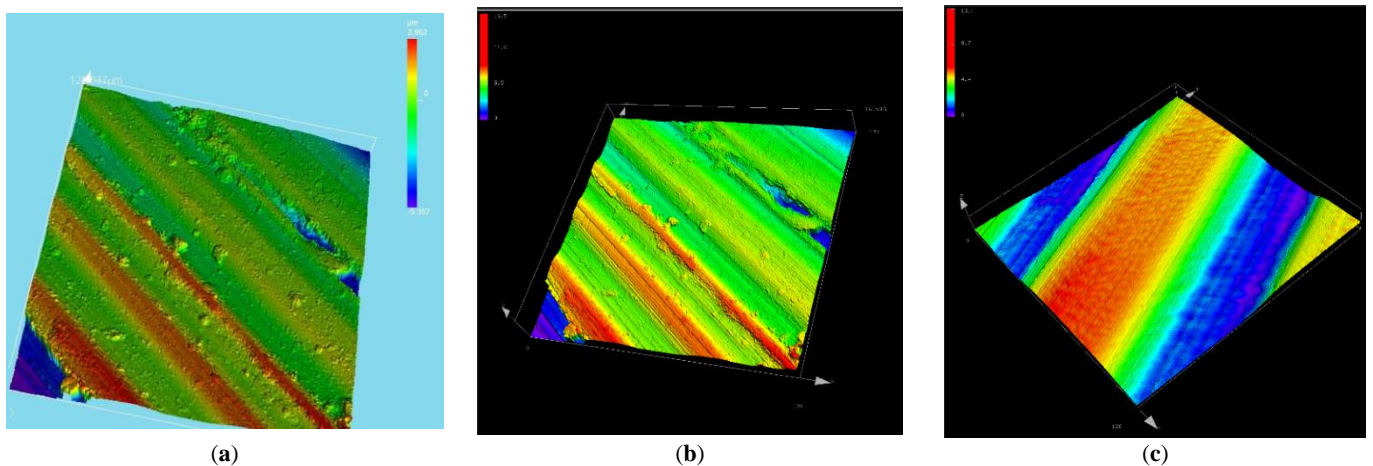


**Figure 9.** 3D profile image of the worn surface of UHMWPE discs: (a) against SN0 pin; (b) against SN20 pin; (c) against SN30.

According to previous studies, we know that the incorporation of hBN would be detrimental to the mechanical properties of silicon nitride ceramic, which might be attributed to the interfacial failure between hBN and  $\text{Si}_3\text{N}_4$  [23]. From Figure 2, it can be clearly seen that the pure  $\text{Si}_3\text{N}_4$  ceramic presents a denser structure. In this study, under SBF lubrication, fracture occurred on the wear surfaces of the  $\text{Si}_3\text{N}_4$ /UHMWPE pair at the beginning stage of the friction process. A part of wear particle would be taken away from the wear interface, while a part of the residual particles would accumulate on the wear surface. Thus, some loose wear debris could be observed on the worn surface of the UHMWPE disc against pure  $\text{Si}_3\text{N}_4$  (Figure 8a). With the increase of hBN content, more fracture and spalling occurred on the wearing surface of the  $\text{Si}_3\text{N}_4$ -hBN/UHMWPE pair. Even though some

wear particles were taken away by the SBF fluid, more and more particles adhered to the wear surface (Figure 8b,c). When hBN content reached 20%, a balance between the residual particles and spalling pits were reached. Namely, the residual particles mainly deposited in the spalling pits, and reacted with SBF lubricants. The tribochemical products provided a protected and lubricated effect for the sliding pair, and lower friction and wear were obtained. When hBN content further increased, the surface of ceramic pin was too rough, and serious mechanical wear was the main wear mechanism.

In recent years, a lot of scholars have been working on the research of bio-tribology of bone implants. Samanta et al. [29] found the wear rate of multilayer Ti/TiN coating against UHMWPE was  $8 \times 10^{-5} \text{ mm}^3/\text{Nm}$  for bio-tribological application. Liu et al. [30] also indicated that Zr/a-C GMFs exhibited the lowest friction coefficient at 0.114, and a wear rate of  $1.47\text{--}1.56 \times 10^{-5} \text{ mm}^3/\text{Nm}$ . Meanwhile, Sahasrabudhe et al. [31] found that the multi-material Ti6Al4V-calcium phosphate-nitride coatings show a lower friction coefficient of 1.25 and a wear rate of  $2.71 \times 10^{-4} \text{ mm}^3/\text{Nm}$ . Obviously, compared with these finding, the tribological properties of silicon nitride matrix composite ceramics need to be further improved. Moreover, this paper only focused on the tribological performance in the SBF environment, and failed to pay sufficient attention to the potential effect of lubricant composition, protein adsorption, contact conformity and transient operating conditions (which are all important factors in biologic tribology [32–34]). Thus, in the later stage, the relevant research work will be carried out.

#### 4. Conclusions

In this study, the bio-tribological performances of  $\text{Si}_3\text{N}_4$ -hBN/UHMWPE bearing pair under SBF lubrications were investigated. The following research findings were obtained.

- The optimal friction pair is  $\text{Si}_3\text{N}_4$ -20%hBN/UHMWPE. In such a setting, excellent bio-tribological performance was obtained. Too much or too little hBN content will lead to the wear of the UHMWPE disc.
- Tribochemical behaviors contributed greatly to good bio-tribological properties. In SBF lubricate, due to interfacial failure between hBN and  $\text{Si}_3\text{N}_4$ , some tribochemical products were formed in the wear pits. The products could play a continuous and stable lubrication role.

The bio-tribological information from the study can promote the utilization of  $\text{Si}_3\text{N}_4$ -20%hBN/UHMWPE pair in the design of artificial joint prosthesis.

**Author Contributions:** Conceptualization, H.L. and W.C.; methodology, L.Z.; validation, H.S., C.Z. and X.L.; formal analysis, H.S.; investigation, H.S.; writing—original draft preparation, H.L.; writing—review and editing, W.C.; supervision, L.Z.; project administration, W.C.; funding acquisition, W.C. All authors have read and agreed to the published version of the manuscript.

**Funding:** This research received funding provided by Natural Science Foundation of Shaanxi Province, China (Grant No. 2018JM5056).

**Institutional Review Board Statement:** Not applicable.

**Informed Consent Statement:** Not applicable.

**Data Availability Statement:** Not applicable.

**Conflicts of Interest:** The authors declare no conflict of interest.

#### References

1. Gergo Merkely, M.D.; Jakob Ackermann, M.D.; Christian Lattermann, M.D. Articular cartilage defects: Incidence, diagnosis, and natural history. *Oper. Tech. Sports Med.* **2018**, *26*, 156–161. [[CrossRef](#)]
2. Learmonth, I.D.; Young, C.; Rorabeck, C. The operation of the century: Total hip replacement. *Lancet* **2007**, *370*, 1508. [[CrossRef](#)]
3. Malchau, H.; Herberts, P.; Eisler, T.; Garellick, G.; Soderman, P. The Swedish total hip replacement register. *J. Bone Jt. Surg. Am.* **2002**, *84*, 2–20. [[CrossRef](#)]
4. Ingham, E.; Fisher, J. Biological reactions to wear debris in total joint replacement. *Proc. Inst. Mech. Eng.* **2000**, *214*, 21–37. [[CrossRef](#)] [[PubMed](#)]

5. Ingham, E.; Fisher, J. The role of macrophages in osteolysis of total joint replacement. *Biomaterials* **2005**, *26*, 1271–1286. [[CrossRef](#)] [[PubMed](#)]
6. Si, Q.Z.; An, X.L.; An, Y.F. Medical ultra-high molecular weight polyethylene modification and tribological characteristics. *Chin. J. Tissue Eng. Res.* **2013**, *17*, 496–500.
7. Gerber, T.; Traykova, T.; Henkel, K.O. Development and in vivo test of sol-gel derived bone grafting materials. *Sol-Gel Sci. Technol.* **2003**, *26*, 1173–1178. [[CrossRef](#)]
8. Zhang, X.; Meng, S.; Huang, Y.; Xu, M.; He, Y.; Lin, H.; Han, J.; Chai, Y.; Wei, Y.; Deng, X. Electrospun gelatin/beta-TCP composite nanofibers enhance osteogenic differentiation of BMSCs and in vivo bone formation by activating Ca(2+)-sensing receptor signaling. *Stem Cells Int.* **2015**, *2015*, 507154. [[CrossRef](#)] [[PubMed](#)]
9. Gwo-Chin, L.; Raymond, H.K. Incidence of modern alumina ceramic and alumina matrix composite femoral head failures in nearly 6 million hip implants. *Arthroplasty* **2017**, *32*, 546–551.
10. Soon, G.; Belinda, P.M.; Lai, K.W.; Akbar, S.A. Review of zirconia-based bioceramic: Surface modification and cellular response. *Ceram. Int.* **2016**, *42*, 12543–12555. [[CrossRef](#)]
11. Carrasquero, E.; Bellosi, A.; Staia, M.H. Characterization and wear behavior of modified silicon nitride. *Int. J. Refract. Met. Hard. Mater.* **2005**, *23*, 391–397. [[CrossRef](#)]
12. Pettersson, M.; Tkachenko, S.; Schmidt, S.; Berlind, T.; Jacobson, S.; Hultman, L.; Engqvist, H.; Persson, C. Mechanical and tribological behavior of silicon nitride and silicon carbon nitride coatings for total joint replacements. *J. Mech. Behav. Biomed. Mater.* **2013**, *25*, 41–47. [[CrossRef](#)] [[PubMed](#)]
13. Bal, B.S.; Khandkar, A.; Lakshminarayanan, R.; Clarke, L.; Hoffman, A.A.; Rahaman, M.N. Fabrication and testing of silicon nitride bearings in total hip arthroplasty: Winner of the 2007 “HAP” PAUL Award. *J. Arthroplast.* **2009**, *24*, 110–116. [[CrossRef](#)]
14. Saito, T.; Imada, Y.; Honda, F. Chemical influence on wear of Si<sub>3</sub>N<sub>4</sub> and hBN in water. *Wear* **1999**, *236*, 153–158. [[CrossRef](#)]
15. Wang, R.G.; Pan, W.; Jiang, M.N.; Chen, J.; Luo, Y.M. Investigation of the physical and mechanical properties of hot-pressed machinable Si<sub>3</sub>N<sub>4</sub>/h-BN composites and FGM. *Mater. Sci. Eng.* **2002**, *B90*, 261–268.
16. Kusunose, T. *Innovative Processing and Synthesis: Ceramic, Glass and Composite*; American Ceramic Society: Westerville, OH, USA, 1997; pp. 443–454.
17. Skopp, A.; Woydt, M.; Habig, K.H. Unlubricated sliding friction and wear of various Si<sub>3</sub>N<sub>4</sub> pairs between 22 °C and 1000 °C. *Tribol. Int.* **1990**, *23*, 189–199. [[CrossRef](#)]
18. Carrapichano, J.M.; Gomes, J.R.; Sliva, R.F. Tribological behaviour of Si<sub>3</sub>N<sub>4</sub>-BN ceramic materials for dry sliding applications. *Wear* **2002**, *253*, 1070–1076. [[CrossRef](#)]
19. Chen, W.; Gao, Y.M.; Chen, C. Tribological characteristics of Si<sub>3</sub>N<sub>4</sub>-hBN ceramic materials sliding against stainless steel without lubrication. *Wear* **2010**, *269*, 241–248. [[CrossRef](#)]
20. Chen, W.; Wang, K.; Liu, X. Investigation of the friction and wear characteristics of Si<sub>3</sub>N<sub>4</sub>-hBN ceramic composites under marine atmospheric environment. *Int. J. Refract. Met. Hard Mater.* **2019**, *81*, 345–357. [[CrossRef](#)]
21. Chen, W.; Shi, H.X.; Xin, H.; He, N.R.; Yang, W.L.; Gao, H.Z. Friction and wear properties of Si<sub>3</sub>N<sub>4</sub>-hBN ceramic composites using different synthetic lubricants. *Ceram. Int.* **2018**, *44*, 16799–16808. [[CrossRef](#)]
22. Xin, H.; Shi, H.X.; Chen, W. Tribological investigation of Si<sub>3</sub>N<sub>4</sub>-hBN on HXLPE bearing couple: Effects of sliding velocity and contact load. *Ceram. Int.* **2019**, *45*, 6296–6302. [[CrossRef](#)]
23. Chen, W.; Gao, Y.M.; Wang, Y.; Li, H.Q. Tribological behavior of Si<sub>3</sub>N<sub>4</sub>-hBN ceramic materials without lubrication under different test modes. *Tribol. Trans.* **2010**, *53*, 787–798. [[CrossRef](#)]
24. Grupp, T.M.; Meisel, H.J.; Cotton, J.A.; Schwiesau, J.; Fritz, B.; Blömer, W.; Jansson, V. Alternative bearing materials for intervertebral disc arthroplasty. *Biomaterials* **2010**, *31*, 523–531. [[CrossRef](#)] [[PubMed](#)]
25. Kokubo, T.; Takadama, H. How useful is SBF in predicting in vivo bone bioactivity. *Biomaterials* **2006**, *27*, 2907–2915. [[CrossRef](#)]
26. Xin, H. *Evaluation of Poly-Ether-Ether-Ketone (PEEK) for Cervical Disc Replacement Devices*; University of Birmingham: Birmingham, UK, 2014; pp. 1–206.
27. Xin, H.; Shepherd, D.E.T.; Dearn, K.D. A tribological assessment of a PEEK based self-mating total cervical disc replacement. *Wear* **2013**, *303*, 473–479. [[CrossRef](#)]
28. Chen, W.; Gao, Y.M.; Ju, F.L.; Wang, Y. Tribochemical behavior of Si<sub>3</sub>N<sub>4</sub>-hBN ceramic materials with water lubrication. *Tribol. Lett.* **2010**, *37*, 229–238. [[CrossRef](#)]
29. Samanta, A.; Rane, R.; Kundu, B.; Chanda, D.K.; Ghosh, J.; Bysakh, S.; Jhala, G.; Joseph, A.; Mukherjee, S.; Das, M.; et al. Bio-tribological response of duplex surface engineered SS316L for hip-implant application. *Appl. Surf. Sci.* **2020**, *507*, 145009. [[CrossRef](#)]
30. Liu, D.G.; Yang, T.T.; Ma, H.R.; Liang, Y. The microstructure, bio-tribological properties, and biocompatibility of titanium surfaces with graded zirconium incorporation in amorphous carbon bioceramic composite films. *Surf. Coat. Technol.* **2020**, *385*, 125391. [[CrossRef](#)]
31. Sahasrabudhe, H.; Bandyopadhyay, A. In situ reactive multi-material Ti6Al4V-calcium phosphate-nitride coatings for bio-tribological applications. *J. Mech. Behav. Biomed. Mater.* **2018**, *85*, 1–11. [[CrossRef](#)]
32. Nečasa, D.; Vrbka, M.; Urbana, F.; Gallob, J.; Krupka, I.; Hartla, M. In situ observation of lubricant film formation in THR considering real conformity: The effect of diameter, clearance and material. *J. Mech. Behav. Biomed. Mater.* **2017**, *69*, 66–74. [[CrossRef](#)]

- 
33. Myant, C.; Fowell, M.; Cann, P. The effect of transient motion on Isoviscours-EHL films in compliant, point, contacts. *Tribol. Int.* **2014**, *72*, 98–107. [[CrossRef](#)]
  34. Nečasa, D.; Vrbkaa, M.; Křupkaa, I.; Hartla, M. The effect of kinematic conditions and synovial fluid composition on the frictional behavior of materials for artificial joints. *Materials* **2018**, *11*, 767. [[CrossRef](#)] [[PubMed](#)]